Application of Boundary Element Modelling to Soft Nips in Rolling Contact

M.F.J. Bohan, T.C. Claypole, D.T. Gethin and S.B. Basri

Abstract

Numerical models have been used to advance the design, predict the performance and develop ink transfer algorithms for printing and coating processes. One of the most generic and difficult areas to successfully model is the nip region of the process. This paper describes a boundary element method to model the interaction between the fluid and soft elastomeric layer in a soft nip in rolling contact as found in printing and coating systems. Case studies of direct relevance to printing are used to demonstrate the efficiency of the approach and its numerical robustness. They are used to highlight the main system design and process operating parameters for ink transfer in printing press nips.

1.0 Introduction

Many printing and coating processes incorporate a series of rollers arranged in a train, which are used to transfer the fluid onto a base substrate in a controlled manner. The roller pairs consist of a solid roller (e.g. steel, copper coated) and a second comprising a solid core element (steel) covered with a soft elastomeric material, Figure 1. These cylindrical pairs operate in a rolling motion, with lateral sliding in certain instances. The engagement between the two rollers give rise large deformation of the elastomer, with relatively low levels of force due to the low elastomer modulus.

A pressure field is generated as the ink flows between the roller pair. The elastomeric surface will deform due to the pressure field and this deformation in turn will affect the pressure in the nip contact. The problem is therefore defined as that of Soft Elasto Hydrodynamic Lubrication (SEHL) in a line contact.

Studies that are both theoretical and experimental in nature have been reported in the literature. One of the first studies [1] was developed for a dry contact condition and was used as basis for some of the subsequent work. The integral equations for the pressure profiles of hard and soft discs in contact were obtained. This work showed the importance of the layer thickness on the pressure profile and deformation. The solution of the integral equation for infinite plane layers was analysed numerically [2] and the various effects including that of

Poisson's ratio was evaluated. Asymptotic solutions to various contact widths were considered in [3] and more recently the effect of different indentations were evaluated in [4].

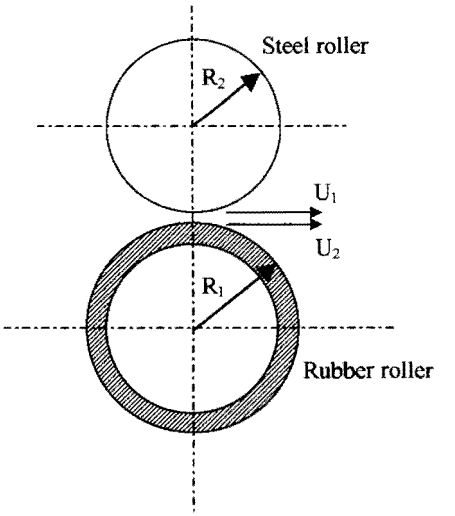

Figure 1 Schematic representation of the roller contact configuration

The lubrication of a layered contact for journal bearings was reported [5], in which the surface indentation was assumed to be proportional to the fluid pressure. The same assumptions were used [6] in analysing a hard roller pair against a polythene target to determine friction and these methods have been further progressed to investigate human joints. Large deformation elastohydrodynamic analysis using inlet / outlet zone analysis is described in [7], with Hertzian pressure dominating at the centre of the contact. This was applied as a technique to reduce the computational time required for the analysis, with the cases considered being that of a cylinder and soft plane surface and a sliding "O" ring seal.

The need to iterate between the fluid and deformation analysis for SEHL is described in [8]. More recently several models have been presented and the different modes of elastohydrodynamic lubrication compared [9]. These modes were dependent upon the flow characteristics at the nip inlet. The application of these techniques to printing has only occurred in recent years [10], [11]. These papers all show a marked difference from the Hertzian pressure and film thickness for both starved and flooded nip contacts. The film thickness determines the ink flow through the system and hence changes will have significant influence on the ink density and final printed image.

This paper focuses on the numerical investigation of the nip contact on a typical offset printing press. A boundary element model has been developed which assumes Newtonian flow in the nip region, which can be expanded to include non-Newtonian flow at a later date and which is more appropriate to the printing and coating processes.

2.0 Governing Equations

In the introduction it was shown the elastohydrodynamic lubrication comes from the coupling of the solution of the Reynolds equation with that of the elastic deformation of the roller

2.1 Reynolds Equation

The governing equation for Newtonian flow away from the edge of the roller provided the contact width is small by comparison with the roller diameter is given by the Reynolds equation below

$$\frac{d}{dx}\left[\frac{h^3}{12\mu}\frac{dp}{dx}\right]=U\frac{dh}{dx} \qquad \ldots 1$$

The assumption of a Newtonian fluid is common to much of the analysis published to date [10], [11], although it has been shown that the ink is non-Newtonian and this has an impact on the pressure field and fluid film thickness [12]. Boundary conditions were applied, such that the pressure at inlet and outlet were set to zero and in addition, the pressure gradient at the outlet was also set to zero to satisfy the Swift Steiber condition. The latter was established automatically within the algorithm and effectively defined the rupture point to satisfy flow continuity.

This equation was solved by the use of Green's function with the right hand side being replaced with the Dirac delta function $\delta(x-\zeta)$. The fundamental solution can be found using the following relationships where

$$g(x,\zeta)=\begin{cases}\int_{\zeta}^{x}\frac{1}{2h^*}dx\ for\zeta>x\\ -\int_{\zeta}^{x}\frac{1}{2h^*}dx\ for\zeta<x\end{cases} \qquad \ldots 2$$

and the differential

$$\frac{dg(x,\zeta)}{dx} = \begin{cases} \dfrac{1}{2h^*} & for \quad \zeta > x \\ -\dfrac{1}{2h^*} & for \quad \zeta < x \end{cases} \qquad \ldots 3$$

and $h^* = h^3$.

By solving equation (1) with the use of equations (2) and (3), an expression for the pressure can be derived where

$$p(\zeta) = \left[h^*(x_1)g(x_1,\zeta), h^*(x_2)g(x_2,\zeta) \right] \begin{bmatrix} v_1 \\ v_2 \end{bmatrix} + \left[h^*(x_1)\frac{dg}{dx}\bigg|_{x=x_1}, -h^*(x_2)\frac{dg}{dx}\bigg|_{x=x_2} \right] \begin{bmatrix} p_1 \\ p_2 \end{bmatrix} + \int_{x_1}^{x_2} \psi(x) \cdot g(x,\zeta) dx \qquad \ldots 4$$

2.2 *Elasticity Equations*

The boundary integral formulation to solve the general boundary problem of elastostatics is given below [13],

$$c_{lk}^i u_k^l + \int_\Gamma p_{lk}^* u_k d\Gamma = \int_\Gamma u_{lk}^* p_k d\Gamma + \int_\Omega u_{lk}^* b_k d\Omega \qquad \ldots 5$$

with c_{lk}^i representing the corner factor, u_k the displacement and p_k the traction on the boundary Γ, i representing a point on the boundary Γ and b_k the body forces at any point within the domain Ω. The Kelvin solution of the problem is given for the displacements and traction by u_{lk}^* and p_{lk}^*. For the problem under consideration, the body forces equal zero (no thermal or gravity effects) and the equation can be simplified to become

$$c_{lk}^i u_k^i + \int_\Gamma p_{lk}^* u_k d\Gamma = \int_\Gamma u_{lk}^* p_k d\Gamma \qquad \ldots 6$$

2.3 *Film Thickness Equation*

The film thickness is given by the following, with a negative value of h_0 indicating roller engagement

$$h(x) = h_0 + \frac{x^2}{2R} + u(x) \qquad \ldots 7$$

2.4 Load Equation

Closure of the solution is attained by the pressure load satisfying the following condition

$$\int_{x_1}^{x_2} p \cdot dx = L \qquad \ldots 8$$

3.0 Solution of the equations

The boundary of the elastomer is divided into a number of elements, Figure 2, to obtain the integrals in the elasticity equation (6). Each of these integrals can be represented by the sum of integrals on the boundary elements. The use of linear elements in a finite plane model allows the element integrals to be calculated analytically.

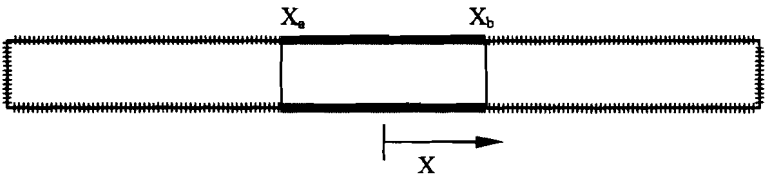

Figure 2 Schematic discretization of boundary layer

Numerical singularities can occur when a field point ζ_0 is located at a node where the integration takes place. These can be eliminated with the use of corner factors and the techniques indicated in [14].

The solution is attained by the following procedure

i. Set an initial value for the engagement, h_0, from this the Hertzian pressure and the consequent indentation is calculated.
ii. The film thickness is calculated in the nip junction.
iii. The film pressure is then calculated.
iv. The indentation was recalculated.
v. If the indentation has not met the convergence criteria, then repeat from stage (ii) with the new indention.
vi. Once the indentation criterion has been meet, examine the load equilibrium. If this is not met then appoint a new value for h_0 and repeat from (i).

4.0 Analysis of printing press contacts

The case studies illustrate the effects of changing press parameters on the computed film pressure profiles and film thickness variation through the nip junction. These finding can be used to assess the sensitivity of the nip contact to these changes. The press parameters used are shown in Table 1 and are typical of those found in many ink train configurations.

Load	Speed	Viscosity	Roller radius	Elastic modulus	Rubber thickness
1500	1.0 ms^{-1}	4 Pa.s	Roll 1 - 0.045 Roll 2 - 0.052	2.0e+6 2.0e+11	8 mm

Table 1 Press parameters used numerical model simulation of nip contact

The convergence criteria for the indentation and pressure load were set to 0.1%. The iterative process would normally require approximately 500 steps before convergence was achieved. Due to the ability to separate the traction from the coefficient matrices, it was possible to carry out the large number calculations required relatively quickly. This resulted in the computation being two orders of magnitude faster than the authors had found when using finite element analysis [15].

A comparison of the boundary element model results with those obtained from finite element analysis from [15] is shown in Figure 3, for two roller speeds. The definition of the problem is different for each of the models with the boundary element model requiring a load for the calculations whereas an initial engagement is used in the finite element analysis. The loadings for the boundary element model were calculated from the pressure profiles obtained using the finite element analysis. Identical fluid properties, material properties, operating conditions and roller configurations were used for both sets of numerical analysis. The fluid film thickness results show good agreement with similar profiles and minimum values being calculated using each of the methods, for each of the roller speeds. The film pressures show only reasonable agreement with the different contact widths being calculated for the two methods. As the load is predetermined using the boundary element method the narrowing of the contact width will increase the maximum pressure calculated. However, the trends with increasing speed are in good agreement between the two models, as is the widening of the contact width with increasing speed. The calculation of the contact width remains an area of difficulty with the start position of the fluid film and its rupture. The two models describe the contact width in different ways with the Hertzian width being used as a starting contact width for the boundary element model and a user definition of the width for the finite element analysis.

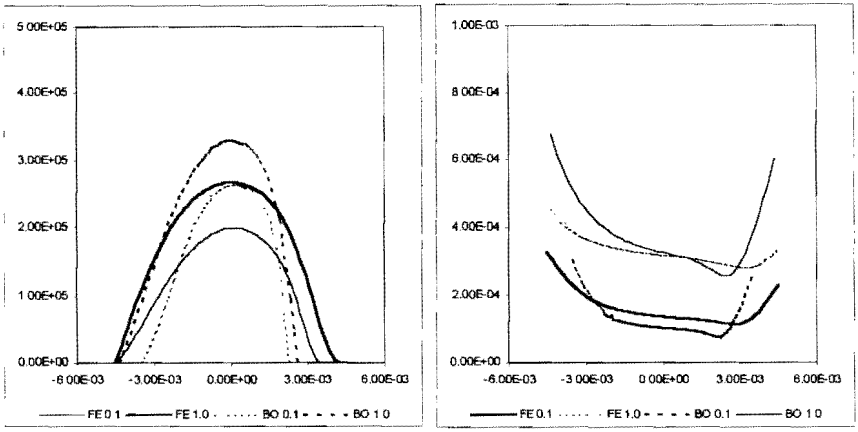

Figure 3 Comparison of film pressure and thickness for finite and boundary element models (Loads = 1017 and 1547 Nm, U = 0.1 and 1.0 ms^{-1}, μ = 6.9 Pa.s, E_r = 2.0 MPa)

With respect to the elastomeric roller, the fixing technique of the rubber sleeve to the steel core is of importance. These are simulated numerically by altering the boundary conditions and fixing either the central or all the nodes on the lower rubber surface, X_a to X_b, Figure 2. The effects of the lower surface being bonded to the steel core and a pressure fit (the latter representing a slip condition) is shown in Figure 4. These show very little difference in either the pressure field or the film thickness. These indicate that for the case under consideration, the rubber fixity has a very small impact, with the lateral movement of the rubber due to the pressure field being minimal. Thus, the following investigations are all shown for the same rubber fixity, that of a bonded interface.

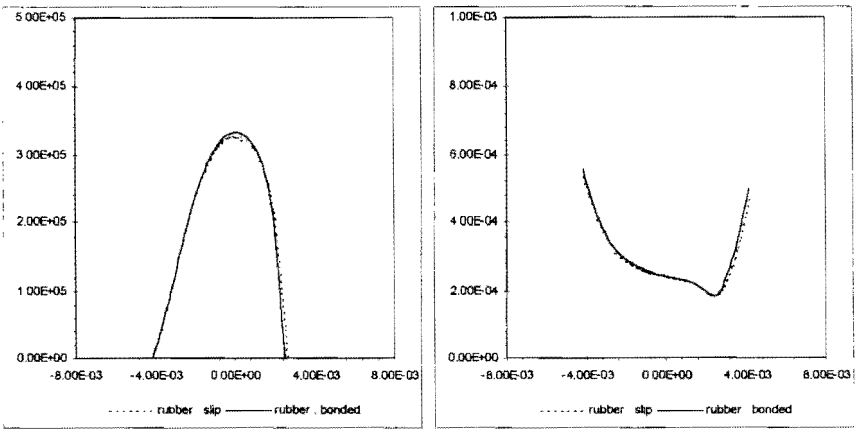

Figure 4 Film pressure and thickness for different rubber fixing (Load = 1500 Nm. U = 1.0 ms^{-1}, μ = 4 Pa.s, E_r = 2.0 MPa)

The influence of increasing the load at the nip junction is shown in Figure 5. These clearly show the maximum pressure increases, as the nip load is increased. In addition, the total width of the contact gets larger with the greater load. The contact width used for the analysis is determined by the Hertzian contact width a, where a is defined as

$$a = \sqrt{\frac{4LR}{\pi E^*}} \qquad \ldots 9$$

Therefore, as the load is increased the contact width will also increase. The start point for all the pressure field analysis is then set to the Hertzian contact width. The shape and form of the film thickness profiles are similar with only small variations in the film thickness at the centre of the nip. However, the rupture point is computed via the Swift-Steiber condition where the nip rupture is shown to increase at the higher pressures, but to a lesser extent in comparison with the film formation point.

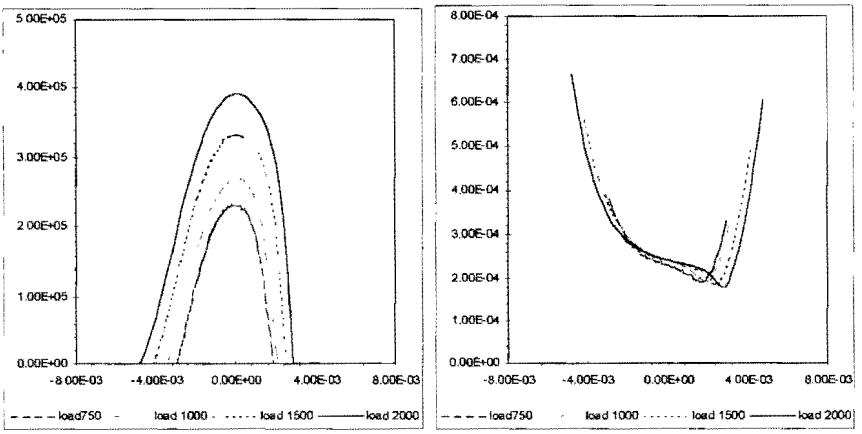

Figure 5 Film pressure and thickness for different roller loadings (U = 1.0 ms^{-1}, μ = 4 Pa.s, E_r = 2.0 MPa)

The film behaviour with respect to different roller speeds is illustrated in Figure 6. These show that for identical loads, only a higher film thickness occurs in the nip junction as the roller speed is increased but with a consequent increase in fluid flow through the nip as a results of both speed and film thickness. These findings are in good agreement with earlier published data [12]. As the speed is increased the maximum pressure in the nip moves slightly towards the entry zone of the contact.

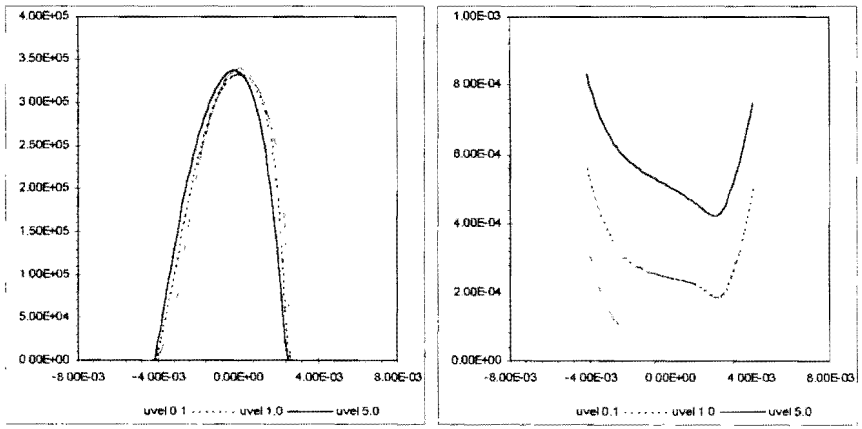

Figure 6 Film pressure and thickness for different press speeds (Load = 1500 Nm, μ = 4 Pa.s, E_r = 2.0 MPa)

The effect of different rubber layer thickness on the elastomeric roller is shown in Figure 7. The reduction in the thickness results in an increase in the maximum pressure carried by the roller pair with the resultant decrease in the contact width. The film thickness profiles are also altered, primarily in their form, with slightly lower film thickness at the outlet calculated with the thinner rubber layer.

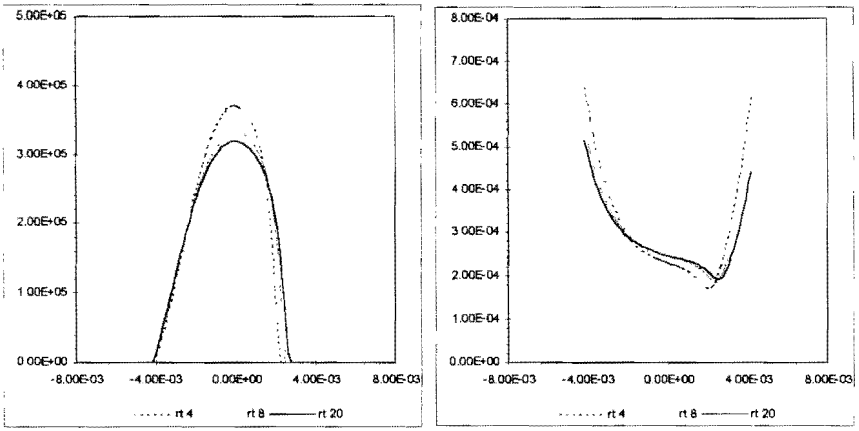

Figure 7 Film pressure and thickness for different rubber thickness (Load = 1500 Nm, U = 1.0 ms^{-1}, μ = 4 Pa.s, E_r = 2.0 MPa)

Figure 8 illustrates the effect of varying the elastomer modulus on the nip junction characteristics. These show a decrease in the film thickness as the rubber modulus is increased with the nip contact width also being reduced. However, the maximum ink film pressure is shown to increase with the increase in rubber modulus. As the elastomer modulus increases the rubber becomes stiffer and the deformation of the rubber layer reduces. The reduction of the deformation will narrow the contact width. The analysis is based on an equal load for each case so as the contact width narrows the maximum film pressure will increase, as exhibited in Figure 8. The larger film pressures will result in a reduction in the fluid film thickness.

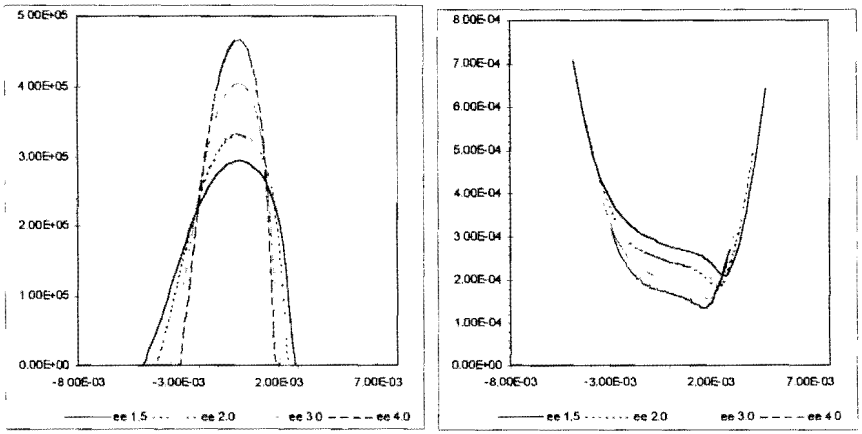

Figure 8 Film pressure and thickness for different rubber modulus (Load = 1500 Nm, U = 1.0 ms^{-1}, μ = 4 Pa.s)

The ink viscosity is shown to have a minimal effect on either the pressure profile or peak value, Figure 9, when varied between 2 Pa.s and 6 Pa.s. In addition there is very little change in the contact width. However, the film thickness is significantly reduced with the decrease in the viscosity levels. These results indicate that changes in the ink viscosity would again affect the ink flow rate through the roller train

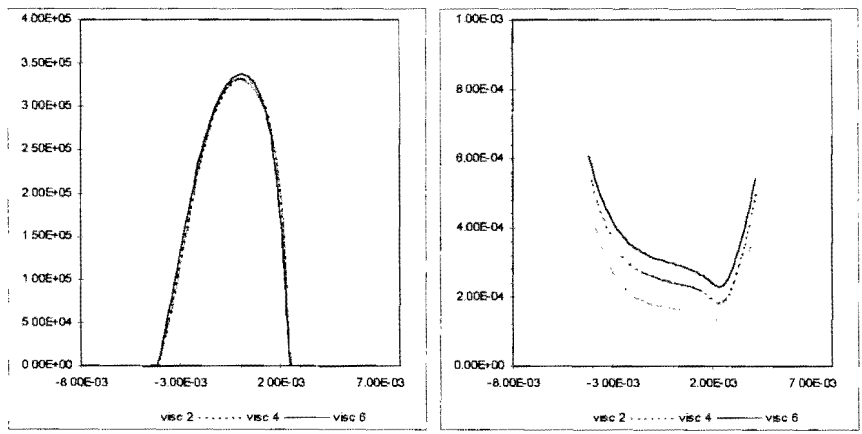

Figure 9 Film pressure and thickness for different fluid viscosity's (Load = 1500 Nm, U = 1.0 ms^{-1}, E_r = 2.0 MPa)

5.0 Conclusions

The boundary element model described in this paper provides a fast and computationally economic solution to the soft elastohydrodynamic problem incorporating a Newtonian fluid. The numerical method is based on the two dimensional elasticity integral equations, therefore possessing the advantage of theoretical strictness. The model can be extended to incorporate a non-Newtonian fluid model into the analysis.

The parametric studies have shown that for the film pressure and thickness

- Increasing roller loading broadened the contact width and increased the maximum pressure.
- Press speed changes affected the film thickness profiles only.
- Reduction in the rubber layer thickness resulted in an increase in the maximum film pressure.
- Increasing the rubber modulus narrowed the contact width, increased the maximum pressure and reduced the film thickness.
- Minimal effect in changing the rubber fixity.

Acknowledgements

The authors wish to thank the European Community for financial assistance throughout this project.

Nomenclature

a	Hertzian contact width
b_k	body forces within boundary domain
c^l_{lk}	corner factor for the boundary integral equation
E^*	equivalent elastic modulus
g	fundamental solution of Reynolds equation
h	fluid film thickness
L	load
p	fluid pressure
p_k	traction for the boundary integral equation
p^*_{lk}	traction for Kelvin solution
p_n	fluid pressure at point x_n
R	equivalent roller radius
U	mean sum of the roller surface velocities
u	surface indentation

u_k displacement for the boundary integral equation

u^*_{lk} displacement for Kelvin solution

v_n pressure gradient $\frac{dp}{dx}$ at point x_n

x co-ordinate for film

Γ boundary surface

δ Dirac delta function

ζ point on the boundary

μ fluid viscosity

ψ term within the Reynolds equation

Ω boundary domain

References

1 Hannah, M. "Contact stress and deformation in a thin elastic layer", Quarterly Journal of Mechanics and Applied Maths, 4, p 94-105, 1951.

2 Miller, R.D.W. "Some effects of compressibility on the indentation of a thin elastic layer by a smooth rigid cylinder", Applied Scientific Research, 16, p 405-424, 1966.

3 Meijer, P., "The contact problem of a rigid cylinder on an elastic layer", Applied Scientific Research, 18, p 353-383, 1968.

4 Jaffar, M.J. and Savage, M.D., "On the numerical solution of line contact problems involving bonded and unbonded strips", Proc. I.Mech.E. Journal of Strain Analysis, 23, p 67-79, 1988.

5 Higgson, G.R. "The theoretical effects of elastic deformation of the bearing liner on journal bearing performance", Proc. Instn. Mech. Engrs., 180, 31-38, 1965-1966.

6 Bennett, J. and Higginson, G.R., "Hydrodynamic lubrication of soft solids", Proc. I.Mech.E. Journal of Mechanical Engineering Sciences, 12, p 218-222, 1970.

7 Hooke, C.J. and O'Donoghue, J.P., "Elastohydrodynamic lubrication of soft, highly deformed contacts", Proc. I.Mech.E., Journal of Mechanical Engineering Sciences, 14, p 34-48, 1972.

8 Cudworth, C.J. "Finite element solution of the elastohydrodynamic lubrication of a compliant surface in pure sliding", 5th Leeds-Lyon Symp. on Tribology, Leeds, 1979.

9 Hooke, C.J. "The elastohydrodynamic lubrication of a cylinder on a elastomeric layer", Wear, Vol. 111, 1986.

10 MacPhee, J., Shieh, J. and Hamrock, B.J., "The Application of Elastohydrodynamic Lubrication Theory to the Prediction of Conditions Existing in Lithographic Printing Press Roller Nips"; Advances in Printing Science and Technology, 21, p 242-276, 1992.

11 Bohan, M.F.J., Lim, C.H., Korochkina, T.V., Claypole, T.C., Gethin, D.T. and Roylance, B.J. "An investigation of the hydrodynamic and mechanical behaviour of a soft nip in rolling contact", Accepted by the IMechE, 1997.

12 Lim, C.H., Bohan, M.F.J., Claypole, T.C., Gethin, D.T. and Roylance, B.J. "A finite element investigation into a soft rolling contact supplied by a non-newtonian ink", J. Phys. D: Appl. Phys, vol. 29, pp 1894-1903, 1996.

13 Brebbia, C.A. and Dominguez, J. "Boundary elements : An introductory course"; McGraw Hill, 1989.

14 Banerjee, P.K. and Butterfield, R. "Boundary element method in engineering science", McGraw Hill, New York, 1981.

15 Claypole, T.C., Gethin, D.T., Lim, C.H., Bohan, M.F.J. and Basri, S.B. "An investigation of rubber roll distortion in a web offset press", 48th Annual TAGA Tech. Conf., Dallas, Texas, April 1996